J.Natn.Sci.Foundation Sri Lanka 2018 46 (4): 527 - 538
DOI: http://dx.doi.org/10.4038/jnsfsr.v46i4.8628

RESEARCH ARTICLE

Modelling the effects of solar activity on the ionospheric F_2 critical frequency over Wakkanai

Muzammil Mushtaq[1*], Faisal Ahmed Khan Afridi[1], Syed Nazeer Alam[2] and Hira Fatima[1]
[1] *Institute of Space and Planetary Astrophysics (ISPA), University of Karachi, Karachi, Pakistan.*
[2] *Department of Electronics and Power Engineering, Pakistan Navy Engineering College, NUST Karachi, Pakistan.*

Revised: 20 March 2018; Accepted: 25 May 2018

Abstract: For many decades ionospheric researchers investigated the variations in the ionosphere due to solar activity. The suggested relevant models are based on single-station data, considering regional and global geographic conditions. The present study investigated the impact of the solar cycles 21st (1976 to 1986) and 23rd (1996 to 2008) on the ionospheric F_2 layer's critical frequency (f_0F_2) at mid-latitude over the Wakkanai region (45.39º N, 141.68º E), Japan. The statistical analyses showed that monthly median f_0F_2 has a significant non-linear association with high sunspot numbers (SSN) over Wakkanai, which represents a saturation effect depending on the time of the day in different months and on the magnitude of the solar cycle. Polynomial empirical models of f_0F_2 based on parameters such as SSN and geomagnetic index A_p were examined. Considering the rate of change in solar activity factor much improved the accuracy of our empirical model and also reduces the hysteresis effect. The most appropriate empirical model for single-station diurnal models of f_0F_2 was developed using Fourier series. Diurnal models incorporate Japanese standard time, months and sunspot numbers. The computed f_0F_2 models were compared with the IRI-2012 model's predicted f_0F_2 values, which demonstrated the better accuracy of the Fourier model compared to the global IRI model. The models obtained in this study are useful for researchers and organisations working in the field of sunspot performance relating to the dynamics of the ionosphere.

Keywords: f_0F_2, geomagnetic A_p index, ionosphere, mid-latitude, sunspot.

INTRODUCTION

The atmosphere of the earth consists of the layers of gases surrounding the earth. Each layer differs in the composition of gas species, altitudes, temperatures and pressures. The Earth's atmosphere extends from 50 km to 1000 km where the solar radiations (especially; EUV and X-rays) highly influence it and create the region of charged particles (positive and electrons). The region where the concentration of charged particles is high enough to reflect the trajectory of radio waves sent from the ground is called the ionospheric layer. The ionosphere lies between 140 km to 600 km in altitude and under certain solar-terrestrial conditions; ionosphere is sub-divided into D, E, F_1, F_2 layers. F_2 layer is the most important region of the ionosphere from the point of view of radio communication and navigation. However, the ionosphere is not a stable ionised medium. The variation of electron density in the F_2 layer possibly enhances or reduces the transmission of a signal propagating at a high frequency between the transmitter and the receiver or it may suddenly interrupt the communication. This disturbance highly depends on the level of solar activity (Sizun, 2003; Jixiang, 2006).

* Corresponding author (muzammilmushtaque@outlook.com; https://orcid.org/0000-0002-3545-1886)

Variation in ionosphere under solar activity

Much effort has been made to study the variations in Earth's ionosphere with respect to different locations on Earth and at different times. Thus, by using ionospheric characteristic data, a large number of stations have developed regional and global models of the ionosphere. These empirical models are established by conducting statistical studies of ionospheric data over a prolonged period. Bilitza (2002) has presented a review of the many available empirical models. Among those models, the international reference ionosphere (IRI) model is broadly used. From different ionospheric parameters, the critical frequency of the F_2 layer (f_0F_2) is one of the most vital parameters that represents the concentration of electron density in the F_2 layer. Critical frequency is defined as the maximum frequency, which is transmitted vertically to the sky and is refracted back to the ground. The f_0F_2 describes the F_2 region of the ionosphere and at night time, f_0F_2 completely explores the F region.

At middle and low latitudes, the solar extreme ultraviolet radiation (EUV) is the primary source of ionisation in the F region (Lakshmi *et al*., 1988). Thus, ionospheric empirical models depend on the high energy radiation coming from the Sun. However, the intensity of EUV and other high energy radiation depends on the magnitude of the solar cycle. As a result of the lack of long-term direct measurements of solar EUV and other high energy radiation, researchers have to rely on other solar activity proxies. X-rays, EUV and UV can be precisely estimated by different solar indices such as sunspot numbers, solar radio flux at 10.7 cm wavelength (F10.7), Mg II core-to-wing index and He 1083 (Maltby & Albregtsen, 1979; Sams III *et al*., 1992; Acton, 1996; Floyd *et al*., 2005; Ramesh & Rohini, 2008; Lukianova & Mursula, 2011; Yan *et al.*, 2011; Usoskin, 2017). The most interesting solar photospheric feature that can be simply observed through a solar telescope in white light are the sunspots, which are the seat of solar activity.

Sunspots initiate as smaller, darker regions on the solar disk which may develop into larger and much darker spots, surrounded by light (dark) regions called penumbrae (Antia *et al.*, 2003). The sunspot number is one of the most commonly used solar proxies because the sunspot number is well correlated to high energy radiation and with other solar proxies. It is convenient to use it because of its long series of observations and its characteristics of reliability and predictability. The solar activity reliance of ionospheric characteristics has been found in early regular ionospheric observations (Richards, 2001; Sethi *et al*., 2002; Atac *et al*., 2009; Maruyama, 2010; Adeniyi & Ikubanni, 2013; Mielich & Bremer, 2013; Elias *et al*., 2014; Ikubanni & Adeniyi, 2017). Earlier researchers suggested the idea about the linear relationship between sunspot numbers and f_0F_2 for every hour and month, which has been frequently used for global, regional as well as single station ionospheric models (De Franceschi & De Santis, 1994; Bilitza, 2001; Holt *et al*., 2002), while after further studying proved that nonlinear relation exists (Pancheva & Mukhtarov, 1998; Ozguc *et al*., 2007; Dabas *et al*., 2008).

IRI model and its uses

International reference ionosphere is a purely empirical standard model of the ionosphere, based on the large collection of ground-based and space observations. It provides monthly average values of ionospheric parameters (such as electron density, ion and electron temperatures, composition of gas species etc.) under the quiet geomagnetic condition (Rawer *et al*., 1978). In the studies, the f_0F_2 data of IRI-2012 (*https://omniweb.gsfc.nasa.gov/vitmo/iri2012_vitmo.html*) model was considered for comparison with the spectral model. The critical frequency F_2 layer directly represented the electron density of the F_2. The highest electron density (N_mF_2) reaches the F_2 peak height (h_mF_2) from where it divides into lower and upper parts. In IRI both parts are normalised to the F_2 peak density and height. Electron density below the F_2 peak is normalised to the E and F_2 peaks. The region between F_1 and F_2 height is of special interest because of its effect on HF radio wave propagation. Electron density (N_e) in that region is described by the IRI function as shown in equation (1),

$$N_e(h) = N_mF_2 \times \frac{\exp(-Z^{B_1})}{\cosh(Z)},\ Z = \frac{h_mF_2 - h}{B_0} \quad ...(1)$$

where the shape of the electron density profile is determined by the lower thickness parameter (B_0) and the shape parameter (B_1). The B_0 is defined as ($B_0 = h_mF_2 - hx$) in which the *hx* is the height where the density profile dropped down to $(0.24 \times N_mF_2)$. The parameters B_0 and B_1 are upgraded every few years by IRI for better description of the global and temporal variation of the ionosphere (Bilitza *et al*., 2014).

In this study, we have illustrated the effects of sunspots on f_0F_2 over Wakkanai. Similar to other models, we have constructed a local-station model of f_0F_2 that usually gives an average value of f_0F_2 incorporating the effect of temporal, seasonal effect, solar cycle and the latitude of the station. It has been observed that specific

models of a particular region are very useful and widely referred to ionospheric services (Pancheva & Mukhtarov, 1998). The diurnal f_0F_2 models for each month for solar maximum and solar minimum years are successfully presented in this study.

METHODOLOGY

From 1948 onwards the ionosonde/digisonde station in Wakkanai has consistently measured ionospheric parameters. These measurements are recorded by the World Data Center (WDC) for Ionosphere and Space Weather in the Japanese city of Tokyo. The center is under the management of the National Institute of Information and Communications Technology (NICT), Japan. The geographic location of Wakkanai is 45.39 °N and 141.68 °E, in the mid-latitude region of Japan. In this research, the hourly data of f_0F_2 in Japanese standard time (JST) and sunspot number were used for the years of 21st and 23rd solar cycles, instead the years of 22nd (1986 – 1996) solar cycle due to the huge deficiency in observational data of f_0F_2. To study the average behaviour of the ionosphere the monthly median hourly values of f_0F_2 were extracted from the entire database, while the missing f_0F_2 values were filled with IRI-2007 model values obtained from the Virtual Ionosphere Thermosphere Mesosphere Observatory (VITMO) (*http://omniweb.gsfc.nasa.gov/vitmo/*). Considering only the effect of seasons, f_0F_2 is independent of solar zenith angle. Generally, f_0F_2 peaks in winter and decreases in summer, and this effect is known as winter anomaly. In the summer season, the enhancement in night-time f_0F_2 called midlatitude summer nighttime anomaly (MSNA) has also been observed over Wakkanai 45º N (Mushtaq *et al*., 2015). The preference of monthly median values over monthly mean values is because of the 27 days solar rotation. The solar rotation has conspicuous variation in EUV radiation, which contributes 85 – 95 % in electron density in the ionosphere (Ruiping *et al*., 2012).

Regression method was used to investigate the dependence of sunspot numbers on the ionospheric F_2 layer (i.e., f_0F_2) over Wakkanai. Regression analysis makes it possible to find the line which best describes the association between two variables. This line is usually referred to as the 'line of best fit' (Jaisingh, 2006). Spectral models explain the complex data as a hypothesis; it predicts the dynamics of f_0F_2 in the frequency domain by observing long-term data records. The diurnal cycles have a significant impact on many phenomena in the Earth's atmosphere, mainly on the ionosphere. To model the complex nature of the ionosphere the spectral approach has been implemented.

For solar proxy, the monthly mean sunspot numbers are used for the said solar cycles given by the Royal Observatory of Belgium located in Uccle, Belgium, which has the geographic position 50.798 °N and 4.358 °E. The relative sunspot number is calculated on the basis of all observations available from different observatories. However, for representing global geomagnetic activity, the monthly mean geomagnetic index A_p is utilised for 1976 – 1986 and 1996 – 2008. Prior to January 1997, data were taken from the Institute fur Geophysik, Gottingen, Germany. Since 1997 up to now, documentation, calculation, and distribution of indices have been moved to Geo Forschungs Zentrum, Helmholtz Center, Postdam, Germany. In this study, data extraction, calculations and plotting were all done in Python 2.7, MATLAB 2015, Easyfit.

RESULTS AND DISCUSSION

Empirical models of f_0F_2 and sunspot number

It is significant to find the empirical models between monthly median hourly f_0F_2 with any best fitted solar proxies. The key parameter used is the sunspot number for ionospheric long-term predictions. Sunspots are one of the best ways to indicate the emission of high energy radiation from the solar surface and its atmosphere (i.e., EUV and X-rays), which are the main sources of ionisation in the ionosphere. We fitted four regression models and to authenticate the correlation of solar activity on f_0F_2, F-test has been performed at 99 % confidence interval which verified that regression analyses between SSN and f_0F_2 are statistically significant for all months. The first regression model is the linear line of best fit. The linear relationships between f_0F_2 and solar proxies have been used in many previous models which are in good agreement with our results (Gulyaeva, 1999; Holt *et al*., 2002; Yanhong *et al*., 2002; Yadav *et al*., 2011). A good linear relation depends on the following situations:

i) It has been found that at moderate sunspot numbers ($60 < SSN < 160$) the linear relation better explained the behaviour of f_0F_2. However, no linear correlation is found at low and high SSN (Ikubanni *et al*., 2013).

ii) In different locations on the Earth, the nature of ionosphere is varying. At equator and low-latitudes the effect of saturation is so strong that no linear relation is suitable for explaining f_0F_2. Mid-latitudes show less variability in f_0F_2 at high SSN, therefore the linear relation can also be considered (Liu *et al*., 2006). Equation (2) describes the linear correlation between the sunspot number and f_0F_2 as,

$$foF2(t)_m = a_{0m}(t) + a_{1m}(t).SSN_m \quad ...(2)$$

where α_0 and α_1 are the coefficients, while t and m show the Japanese standard time in hours and different months, respectively and SSN is the monthly mean sunspot number for the current month. We analysed the relationship at midnight (t = 00 h) and noontime (t = 12 h) in JST, whilst m shows the whole months of a year, and the linear line of best fit is represented as dotted lines as shown in Figures 1 and 2.

At midnight, the linear regression fit seems good in many months, especially around the equinoctial time and the highest adjusted coefficient of determination (adj_R^2) occurred in April (adj_R^2 = 93.7 %), while the lowest adj_R^2 was found in December (i.e., 43.8 %). Higher values of adj_R^2 illustrate that the regression model explains the majority of the variations in f_0F_2 while low values of adj_R^2 show the opposite.

At noontime, linear fits are still a good indication of the relationship between sunspot numbers and f_0F_2, and the maximum and minimum adj_R^2 are 94.8 % and 81.2 % in the months of March and July, respectively. It has been observed that f_0F_2 shows a good linear relationship for low and moderate numbers of sunspots while it shows almost constant or decreasing values at extremely high solar epochs, which is known as the saturation effect. Saturation depends on local hours, months and on the magnitude of the solar cycle. In Figures 1 and 2 it is observed that, in winter, (including the months December and January) the f_0F_2 values show generally constant values of high sunspot numbers, which our first regression model does not demonstrate. Therefore, a better model is expected by using the second regression model, i.e., quadratic relationship between sunspot numbers and f_0F_2 as,

$$foF2(t)_m = b_{0m}(t) + b_{1m}(t).SSN_m + b_{2m}(t).SSN_m^2 \quad ...(3)$$

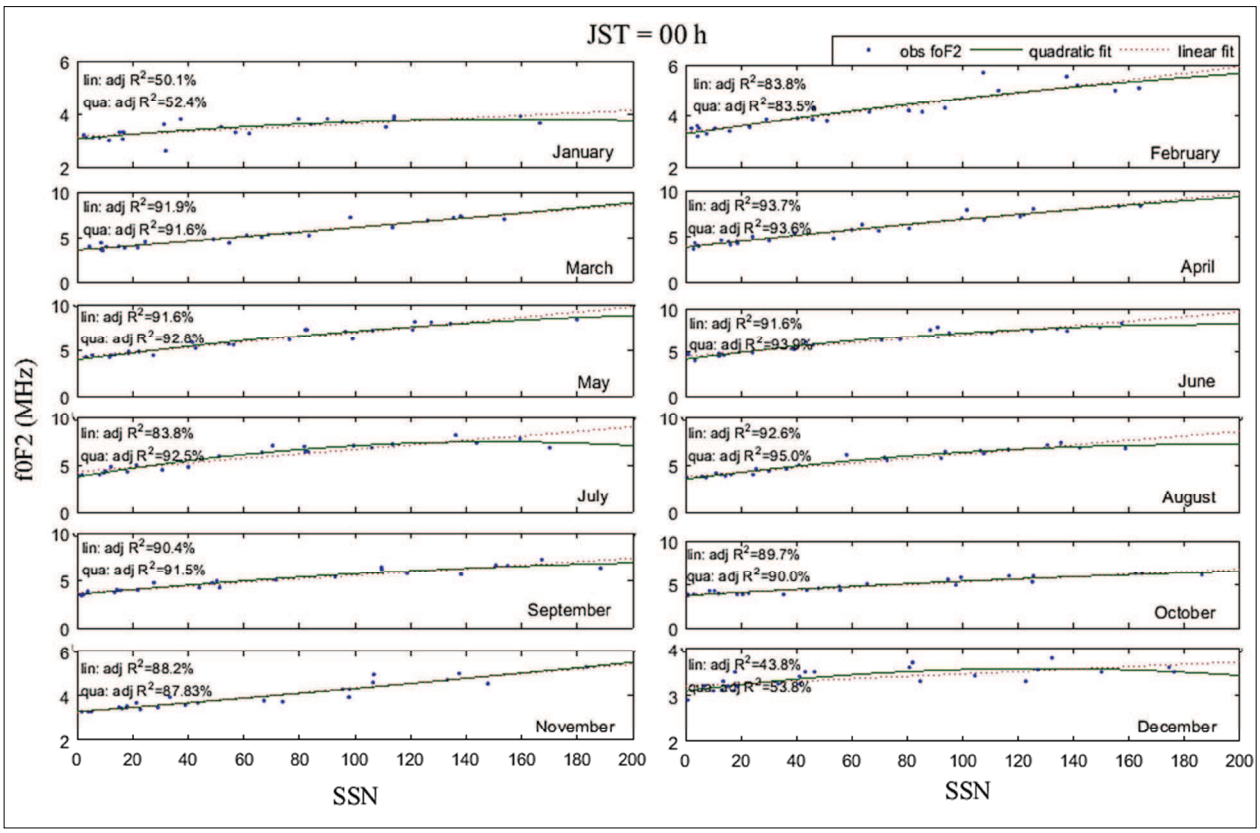

Figure 1: The relationship between monthly median f_0F_2 and monthly mean SSN at JST 0 h for the whole interval of 1976 – 1986 and 1996 – 2008 over Wakkanai. Observed values are plotted as dots, dotted lines represent the linear regression fit while solid lines show the quadratic regression fit.

b_0, b_1 and b_2 are the coefficients of the quadratic regression equation at specified JST time (t) and month (m) represented by a solid line in Figures 1 and 2. In this case the significance of coefficient b_2 is;

i) $b_2 < 0$, indicates that f_0F_2 declines with increasing solar activity, which represents the saturation effect.

ii) $b_2 > 0$, implies that f_0F_2 rises at excessively high solar epochs.

The saturation at noon and midnight in different months is clearly shown by the second regression model in Figures 1 and 2. The maximum difference in adj_R^2 (i.e., 5 and 10 %) is found in December at noon and midnight, respectively. The clear saturation in the noontime monthly median values of f_0F_2 during the winter season (including months of December and January) at Wakkanai (45.39 ºN) is due to the enhancement of the recombination process. Molecular nitrogen (N_2) plays a key role in the recombination process (Rishbeth, 1998). Hedin *et al*. (1979) demonstrated that the density ratio of atomic oxygen and molecular nitrogen (O/N_2) decreases significantly with the increase in solar activity for winter at 45º latitude. This is due to the increase in the scale height of molecular species, especially N_2, rather than the scale height of atomic oxygen at high solar epochs (Schunk & Walker, 1973). This anomalous role of N_2 raises the recombination process, emerging as a saturation effect.

Polynomial regression models of higher orders have been tested, and a good relation between f_0F_2 and SSN at low and moderate sunspot numbers was found. However, randomly steep downward or upward trends at larger sunspot numbers contradicts the actual physical phenomena of the saturation effect. Along with this, the adjusted R^2 also showed no improvement with higher orders.

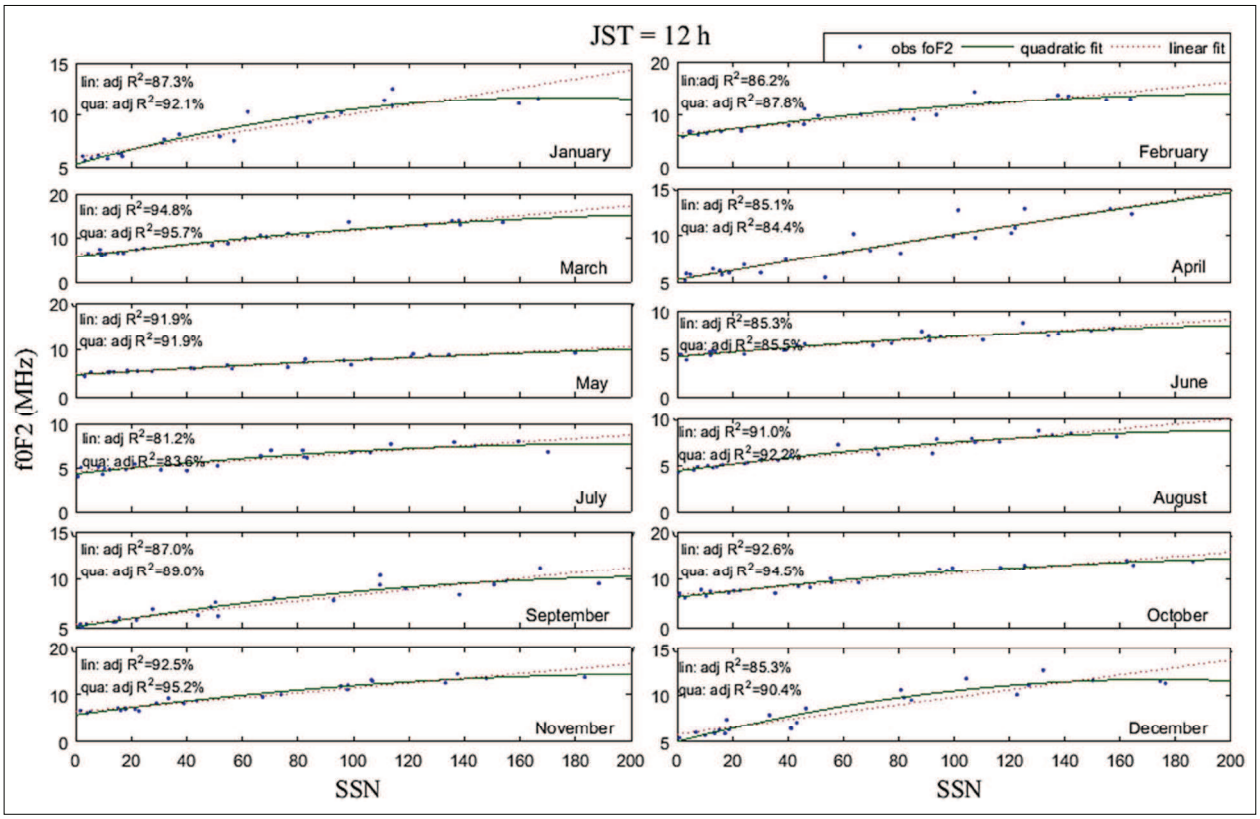

Figure 2: The relationship between monthly median f_0F_2 and monthly mean SSN at JST 12 h for the whole interval of 1976 – 1986 and 1996 – 2008 over Wakkanai. Observed values are plotted as dots, dotted lines represent the linear regression fit while solid lines show the quadratic regression fit.

It has been shown that for lower levels of solar activity, f_0F_2 may vary during ascending and descending parts of the 11-year solar cycles; an effect which is known as the hysteresis effect. This effect is attributed to the activities of geomagnetic storms throughout the solar cycle (Rao & Rao, 1969; Apostolov & Alberca, 1995; Mikhailov & Mikhailov, 1995). The enhanced geomagnetic activity during the declining period of the solar cycle can produce stronger storm effects on the F_2 layer than during the increasing period of the solar cycle. Kane (1992) argued that two key parameters i.e., solar and the geomagnetic index, should be taken into account for long-term prediction models. Therefore, Xu *et al*. (2008) used a multiple regression model by taking two parameters i.e., the sunspot number as solar activity index and geomagnetic index A_p for geomagnetic perturbations of the dependence on the monthly median f_0F_2 over Chongqing, China.

Our analysis of f_0F_2 over Wakkanai (45.39 ºN) supports the model by Kane (1992) that uses both solar and geomagnetic index parameters which improved the regression model. Our third regression model is represented as dashed-square lines in Figure 3 and expressed as,

$$foF2(t)_m = c_{0m}(t) + c_{1m}(t).SSN_m + c_{2m}(t).SSN_m^2 + c_{3m}(t).Ap_m.SSN_m + c_{4m}(t).Ap_m + c_{5m}(t).Ap^2 \quad ...(4)$$

where c_0 to c_5 are the coefficients of the third regression model in a different JST time (t) and month (m) while A_p and SSN are the monthly mean geomagnetic index and sunspot number at the present month, respectively. The coefficients c_1 and c_2 are the quantitative expressions of the current month's sunspot number whilst c_4 and c_5 represent the current month's A_p index values. However, c_3 depicts the combination of solar and geomagnetic disturbances.

The standard deviations of the change in f_0F_2 calculated from regression models and observed values for the years 1976 – 1986 and 1996 – 2008 are illustrated in Figure 3. The diurnal variations of these standard deviations are determined for all months. It is seen that the trend is slightly nearer to zero when using both factors (i.e., solar and geomagnetic index) for the empirical model represented as dashed-square lines. It concludes that the third regression model better explains the observed values rather than the second regression model. The root mean square deviation (RMSD) is often used to measure the difference between two time series trends; RMSD is calculated from the trend of the standard deviations measured from equations (3) and (4). In this scenario, the higher values of RMSD in a specific month indicate that the calculated f_0F_2 values from equation (4) are much closer to the observed values than the f_0F_2 calculated from equation (3) for that particular month. The maximum RMSD was reported in the months of January and July (i.e., 0.049 and 0.0488) and the maximum differences appear at 11:00 and 09:00 hours JST, respectively. Therefore, the third regression model is preferable over the second regression model. However, it is insignificant that in the months of April, May and September, where the RMSD values are the least i.e., 0.0089, 0.017 and 0.0122, respectively.

The hysteresis effect has a great impact on the mid-latitude compared to the low and high-latitudes, which cannot be neglected for empirical and spectral models of f_0F_2, especially at Wakkanai (45º N). Rao and Rao (1969) observed that noontime f_0F_2 values are higher in the decreasing part of the solar cycle while it is low in the rising phase of the solar cycle. This is the consequence of some weak solar activities which can occur with or without sunspot formation because the required magnetic field threshold to form sunspot is 1500 Gauss (Penn & Livingston, 2006). However, the weak magnetic field can produce events such as solar flares, coronal mass ejection, solar winds and energetic protons. Those events occur near or close to the time of formation of sunspots (Legrand & Simon, 1989). High-speed solar wind streams from low solar-latitude coronal holes enhanced much later than sunspots maxima in the falling part of a solar cycle whose effect on ionosphere is even more non-linear (Simon & Legrand, 1986). Therefore in a systematic way, one can consider the rate of change in sunspot numbers for a few-month's time interval from a given month. This approach can potentially cover all the solar activities that occur before and after the formation of sunspots as shown previously by Pancheva and Mukhtarov (1998). Pancheva and Mukhtarov (1998) found that the rate of change in solar activity is low in the descending part of the solar cycle than in the ascending part. The influence of the tendency for a change of solar activity is essential for the years when solar activity varies very rapidly (i.e.; ascending part of the solar cycle). The study (Pancheva & Mukhtarov, 1998) used the Kr parameter and tried to get more accuracy in empirical models, although it is inconvenient because the Kr parameter includes the factor of solar activity after five months from the given month, which may be unknown. Then a new finding was published by Liu *et al*. (2004) in which they only replaced

Kr with F107p (i.e., the prior month's F107 values) as a solar activity parameter over the Wuhan region (30.6 ºN, 114.4 ºE) that gave an even better result. In the present study, SSNp was used (i.e., the monthly mean sunspot number of the previous month). Therefore, the fourth regression model can be given as,

$$foF2(t)_m = d_{0m}(t) + d_{1m}(t).SSN_m + d_{2m}(t).SSN_m^2 + d_{3m}(t).SSNp_m + d_{4m}(t).SSNp_m^2 \quad ...(5)$$

The trend of standard deviations by evaluating equation (5) is represented as a solid line in Figure 3. For all months, it is seen that the fourth regression model has a much lower standard deviation that made it easier to explain the observed f_0F_2 values over Wakkanai. The highest drop in the standard deviation occurs in November from about 0.57 MHz to 0.31 MHz at 08:00 hour JST. For all months, RMSD is computed from the standard deviation trends measured from equations (3) and (5). The RMSD has high values, which is an indication that the best relationship exists between the calculated f_0F_2 from equation (5) with observed f_0F_2, especially in February and September with maximum RMSD value of 0.114 and 0.136, respectively. Introducing SSNp improves the depiction of solar cycle dependence of f_0F_2. In other words, it is observed that the rate of change in solar activity has a significant effect on f_0F_2 over Wakkanai and its response depends on the month and partially on the diurnal cycle as seen in Figure 3. The results demonstrate that the fourth regression model accurately explains the complex behaviour of the ionospheric f_0F_2 parameter.

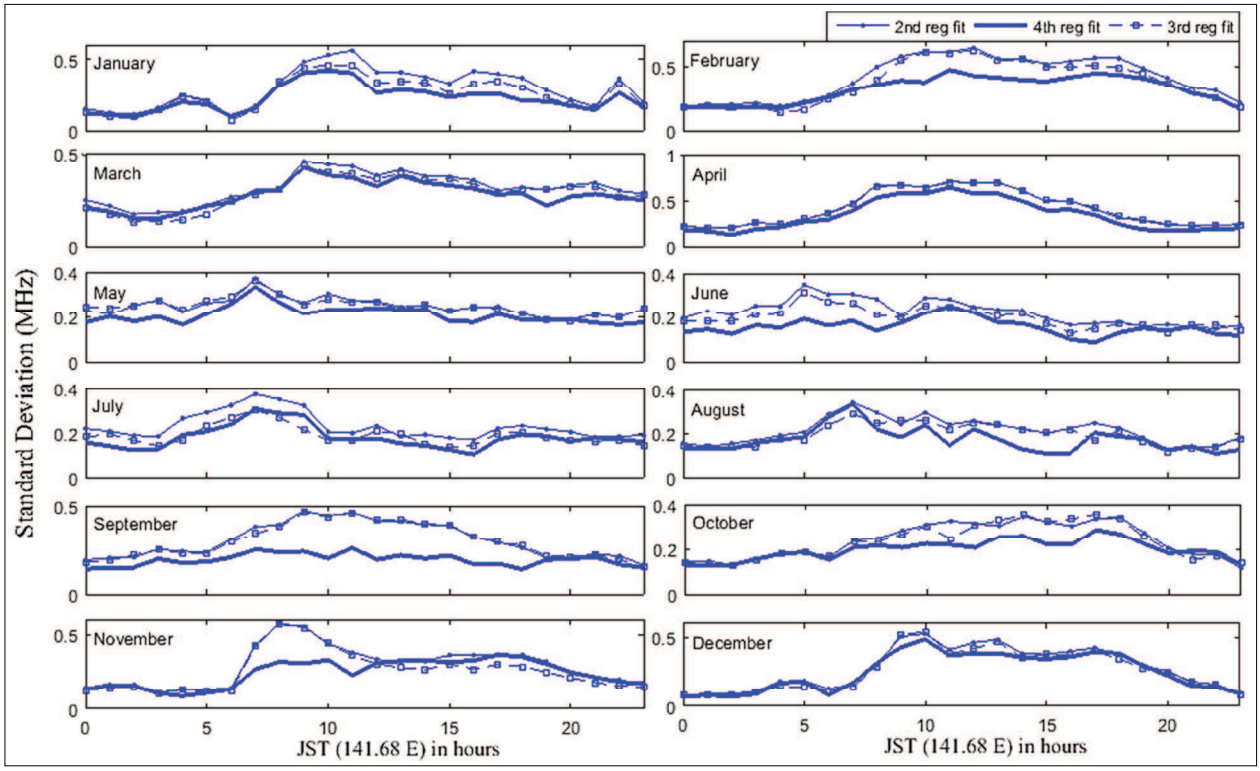

Figure 3: Diurnal variation of the standard deviation of f_0F_2 computed from equations (3), (4) and (5) from the observed f_0F_2 for the whole interval 1976 – 1986 and 1996 – 2008 over Wakkanai. Line dots represent the second regression fit, dashed-square lines show the third regression fit, solid lines are for the fourth regression fit.

Spectral analysis

We have constructed a diurnal f_0F_2 model for Wakkanai 45.39 ºN, based on Fourier series. Four key parameters were used for the model. These are t, m, SSN and SSNp, which represent the diurnal, seasonal and solar cycle variations and the effect of prior solar activity on f_0F_2, respectively, where t is the Japanese standard time, m is

the month, SSN and SSNp are the monthly mean sunspot numbers' value in the specified and previous month, respectively.

Fourier model and its authentication

Fourier series represents periodic functions in terms of cosines and sines. There are diurnal periodicities present in the ionospheric parameters. Therefore, the Fourier series is generally preferred when constructing spectral models. The diurnal variations can be expressed by a Fourier series with periods of 24 hours and higher harmonics. A Fourier series for f_0F_2 can be generally expressed as,

$$foF2(t)_m = x_{0,m} + \sum_{n=1}^{N}\left(x_{n,m}\cos\left(\frac{2\pi nt}{T}\right) + y_{n,m}\sin\left(\frac{2\pi nt}{T}\right)\right) \quad ...(6)$$

where the harmonic number is n (=0, 1, 2, 3…, N), and in our models, we take 4 harmonic numbers to ensure model accuracy and T is equal to 24 hours. The coefficients $x_{n,m}$ and $y_{n,m}$ are functions of SSN and SSNp. These coefficients are computed from equation (6) by using the curve fitting tool in MATLAB software, of the specified months for solar minimum and solar maximum years (i.e., 1976 and 1979, respectively); however, the f_0F_2 values for every month are evaluated from equation (5).

The predicted f_0F_2 values from the Fourier model [i.e., equation (6)] and IRI model are represented as solid lines, whilst the observed f_0F_2 values are symbolised with dots as shown in Figure 4. Left panels are for the Fourier model while right panels are for the IRI-2012 model; both are compared with the observed f_0F_2 values. The solar minimum year (1976) and solar maximum year (1979) were chosen for constructing the f_0F_2 models. For verification of the models, we used the years 1964 and 1968, which are the solar minima and solar maxima years of solar cycle 20, respectively. As f_0F_2 data were missing for the years of solar cycle 22 (1986 – 1996) and 24 (2008 – present), we were unable to work on it. The years used for verification of our models were not included initially in the dataset for regression models. Therefore, the

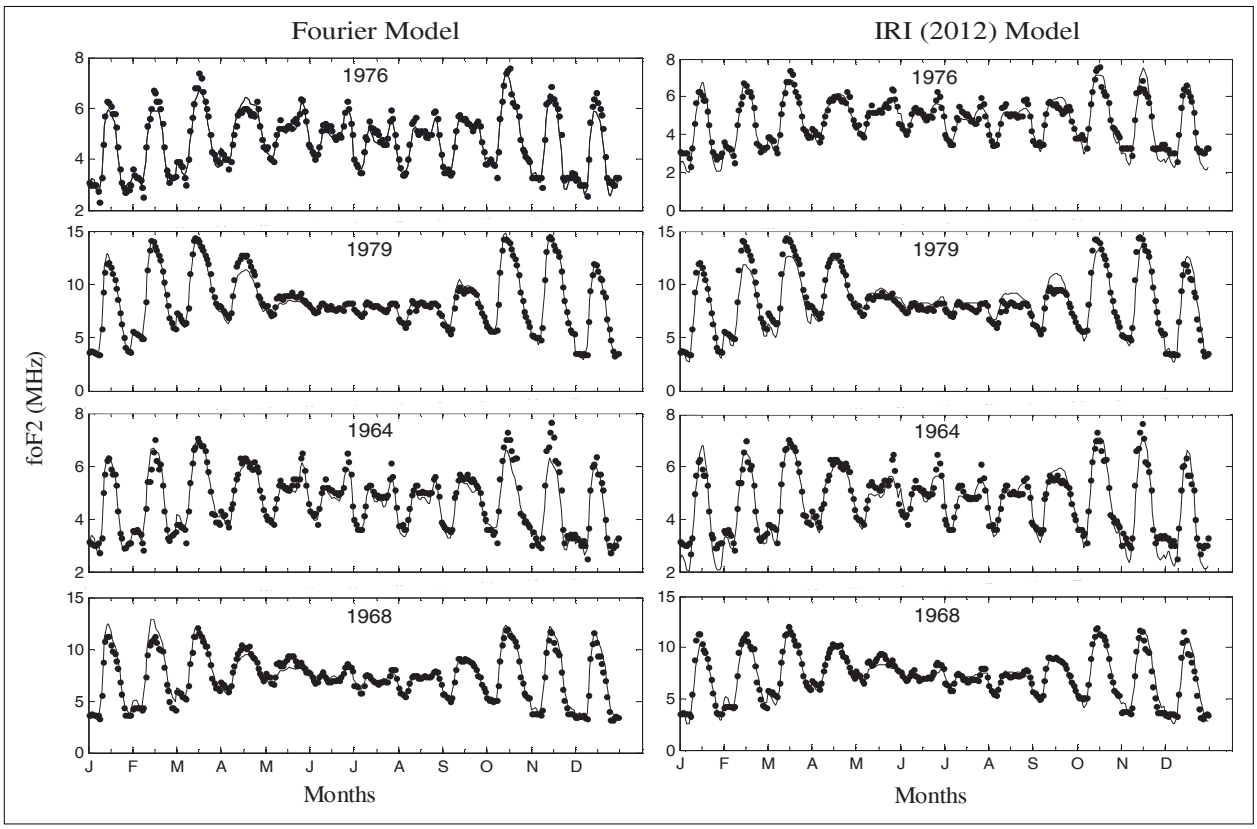

Figure 4: The computed and predicted diurnal variation of the monthly median f_0F_2 represented as solid lines with observed f_0F_2 shown with dots for solar minimum years (1976 and 1964) and for solar maximum years (1979 and 1968).

correctness of our work can be demonstrated by showing the results of the model f_0F_2 values that almost do not change in the years which are not included originally in the dataset for analysis. Hence our Fourier models can be employed for the long-term prediction of the ionospheric f_0F_2 parameter over Wakkanai (45º N).

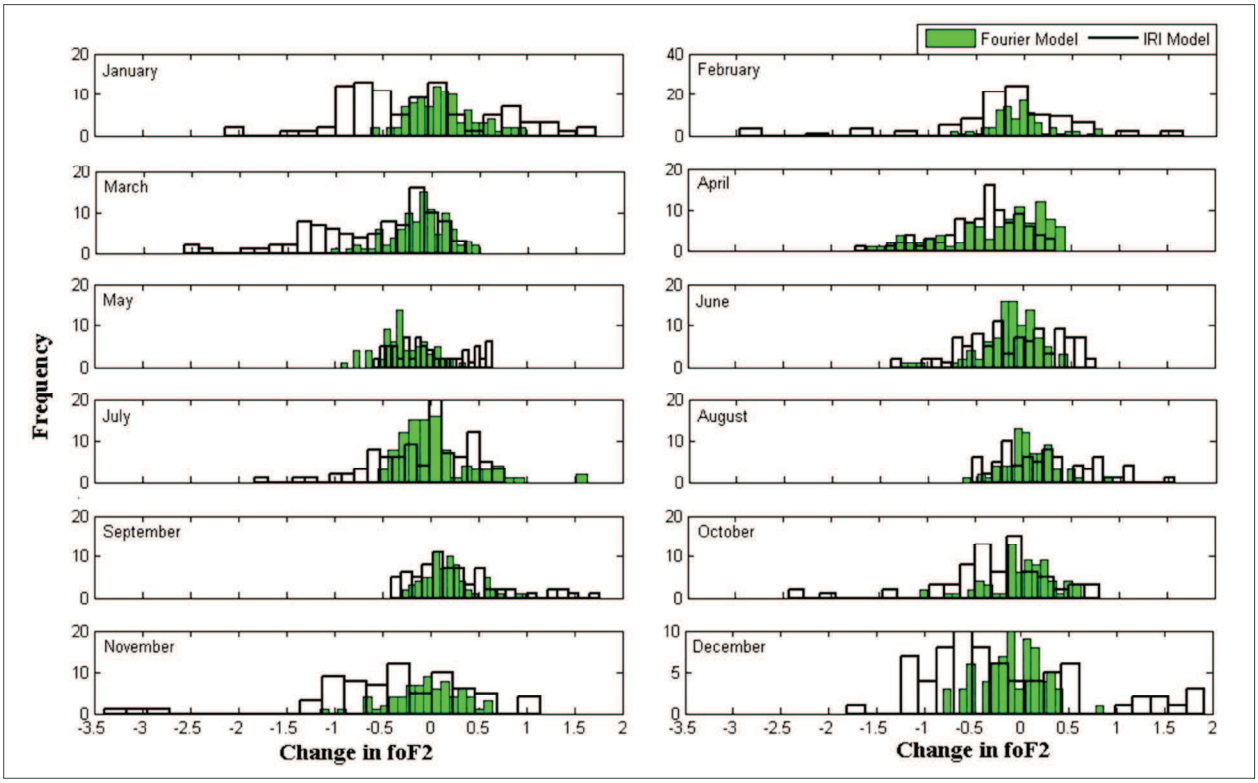

Figure 5: The deviation of computed and predicted (Fourier and IRI-2012) f_0F_2 from observed f_0F_2 for the years 1976, 1979, 1996 and 2000. Green colour bars are for the Fourier model and non-colour bars are for the IRI-2012 model.

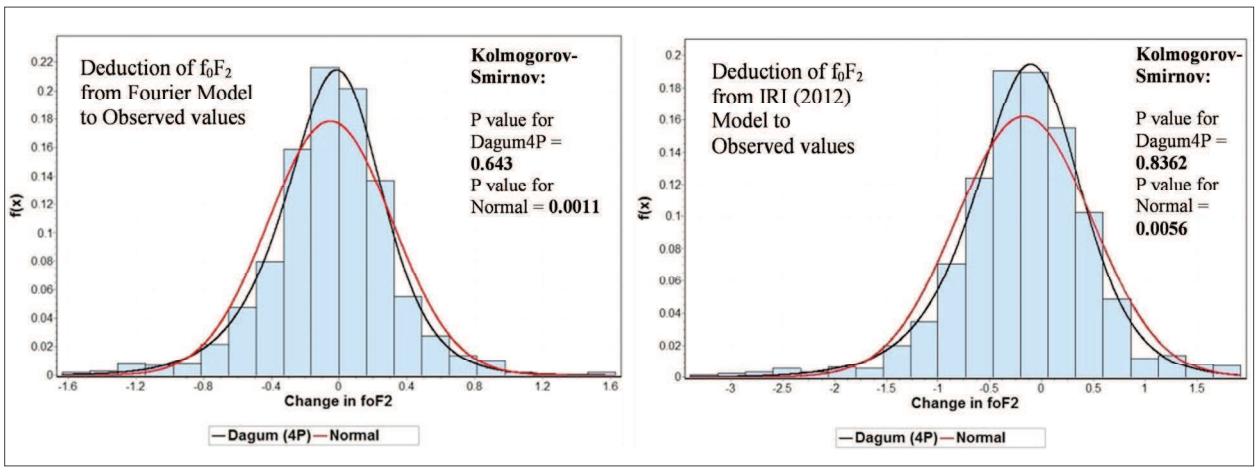

Figure 6: The probability density funtion plot of the change in f_0F_2 of the solar minimum and maximum years of the cycle 21 and 23. The Dagum 4P (in black colour) and normal (in red colour) distributions are fitted.

The deviation of models (Fourier and IRI-2012) from observed f_0F_2 for the solar minimum (1976 and 1996) and maximum (1979 and 2000) years is shown in Figure 5. The missing data of f_0F_2 of the year 2000 for the months of May and August to December are not included in the graph. Figure 5 demonstrates that:

i) Firstly, the deviation of Fourier model f_0F_2 mostly lays closer to zero as shown in the green colour bars, while divergence is much larger for IRI model f_0F_2 as displayed in none colour bars. This illustrates that Fourier model better explains the real behaviour of F2 layer critical frequency than IRI-2012 model over Wakkanai.

ii) Secondly, the estimation of f_0F_2 by Fourier model in the months of April, June and October have more negative values that illustrate our model significantly and underestimate the observed f_0F_2 values while in July and September, model overestimates the f_0F_2 values. Although for all months, the scatter is much higher in the IRI-2012 model as compared to the observed f_0F_2.

The probability density functions (PDF) of the change in f_0F_2 values are plotted in Figure 6, where the frequency on the y-axis shows the probability that x-axis can occupy between two maxima. It explained that high frequency peak near zero means observed f_0F_2 values are close to the calculated (or IRI) f_0F_2 values and low frequency shows opposite behaviour. The peak frequency near to zero is accurately represented by Dagum type II (4P) distribution that is also compared with the normal distribution. The Dagum 4P distribution is a heavy-tail distribution that contains four parameters; two parameters describe the shape, one is for scale and last is the location parameter. The Dagum 4P is frequently used in economic problems in which null and negative data have assets, and it is highly applicable in the cases of extreme data values that are not supposed to be neglected. In our case, comparison of models gives high frequencies with long-tail that are fully explained by the Dagum 4P distribution besides normal distribution that partially explained peak frequency with overestimating frequency at the second-standard deviation of the mean (Kleiber, 2007; Benjamin *et al*., 2013). The p-value test has preferred the Dagum 4P distribution and aborted the normal distribution fitting. PDF reveals that the IRI model is scattered more and under estimate f_0F_2 values from observed values with respect to the Fourier model.

As a worldwide empirical model, the IRI model is outstanding at many spatial locations in the Earth's ionosphere. However, the behaviour of the ionosphere is extremely complex and it changes in different latitudes. We worked on single-station empirical models so the effects of solar activity on f_0F_2 over Wakkanai 45 ºN are highly considered that enabled us to precisely measure the saturation and hysteresis effects and include them in models. A similar methodology has been applied by Liu *et al*. (2004) over Wuhan 30.7 ºN and by Xu *et al.* (2008) over Chongqing 29.56 ºN, China. Therefore, the Fourier model provides much higher accuracy as compared to the IRI model over Wakkanai 45 ºN.

CONCLUSION

The non-linear relationship between f_0F_2 and SSN depends on the time of a day, season-months and the magnitude of solar activity. However, a quadratic regression fit is still better for all months to explain the small variations and especially the saturation effects.

To reduce the hysteresis effect, integrated factors of geomagnetic index A_p and SSN are used, which improved the empirical relationship. However, the relation is still lacking, especially in the months of April, May and September, while introducing prior month sunspot numbers (i.e., SSNp) with current month SSN significantly improved the relationship between solar cycle variation and its influence on f_0F_2 over Wakkanai. The tendency of change in solar activity factor makes the empirical model more appropriate than other regression models and it is suitable to use equation (5) for the spectral models of f_0F_2.

Spectral models are constructed using Fourier series for the solar minimum and solar maximum years (1976 and 1979). A good agreement has been found between the computed f_0F_2 from our models and the observed f_0F_2. We applied our models to the years 1964 and 1968 showing the solar minimum and solar maximum years. Comparable predictions of f_0F_2 from the IRI-2012 model were also analysed. From Figures 5 and 6, it can be seen that the accuracy of our Fourier model is better than the IRI-2012 model, while the IRI model largely underestimated the f_0F_2 values from observed values. The implementation of the Dagum 4P distribution is appropriate to model high frequencies and extreme values. The Dagum distribution is an appealing choice for modelling extreme values when using maximum likelihood estimators.

The Fourier models can be used as a relevant tool to study the effect of sunspot numbers on the F layer of ionosphere during solar minimum and solar maximum periods and it can be also used as a reference for predictions of the f_0F_2 parameter.

Acknowledgement

All researchers of this paper are thankful for Virtual Ionosphere Thermosphere Mesosphere Observatory (VITMO) for providing the IRI 2007 and 2012 model values of f_0F_2. The sunspot number data are downloaded from the Solar Influence Data Center (*http://sidc.oma.be/*). The source of the geomagnetic index is GeoForschungsZentrum, Helmholtz Center, Postdam, Germany. The f_0F_2 data over Wakkanai station is made available from the World Data Center for Ionosphere and Space Weather, Tokyo, Japan, National Institute of Information and Communications Technology *http://wdc.nict.go.jp/IONO/wdc/index.html*.

REFERENCES

Acton L. (1996). Comparison of YOHKOH X-ray and other solar activity parameters for November 1991 to November 1995. In: Cool Stars, Stellar Systems, and the Sun. *Proceedings of the 9th Cambridge Workshop* (eds. R. Pallavicini & A.K. Dupree), volume 109, Florence, Italy, 3 – 6 October, Astronomical Society of the Pacific (ASP), p. 45.

Adeniyi J.O. & Ikubanni S.O. (2013). Determination of the threshold value of F10.7 in the dependence of foF2 on solar activity. *Advances in Space Research* **51**: 1709 – 1714. DOI: http://doi.org/10.1016/j.asr.2012.12.005

Antia H.M., Bhatnagar A. & Ulmschneider P. (2003). *Lectures on Solar Physics*. Springer Verlag, Berlin Heidelberg, Germany.

Apostolov E.M. & Alberca L.F. (1995). foF2 hysteresis variations and the semi-annual geomagnetic wave. *Journal of Atmospheric and Terrestrial Physics* **57**: 755 – 757.

Atac T., Atila O. & Pektas R. (2009). The variability of foF2 in different phases of solar cycle 23. *Journal of Atmospheric and Solar-Terrestrial Physics* **71**(5): 583 – 588. DOI: http://doi.org/10.1016/j.jastp.2009.01.004

Benjamin S.M., Humberto V.H. & Barry C.A. (2013). Use of the Dagum distribution for modeling tropospheric ozone levels. *Journal of Environmental Statistics* **5**(5): 1 – 11.

Bilitza D. (2001). International reference ionosphere 2000. *Radio Science* **36**(2): 261 – 275.

Bilitza D. (2002). Ionospheric models for radio propagation studies. *Review of Radio Science* (ed. W.R. Stone), pp. 625 – 679. IEEE and Wiley Press.

Bilitza D., Altadill D., Zhang Y., Mertens C., Truhlik V., Richards P., McKinnell L-A. & Reinisch B. (2014). The international reference ionosphere 2012 - a model of international collaboration I. *Journal of Space Weather and Space Climate* **4**(2014): Article number A07. DOI: http://doi.org/10.1051/swsc/2014004

Dabas R.S., Sharma K., Das R.M., Sethi N.K., Pillai K.G.M. & Mishra A.K. (2008). Ionospheric modeling for short- and long-term predictions of F region parameters over Indian zone. *Journal of Geophysical Research: Space Physics* **113**(3): A03306. DOI: http://doi.org/10.1029/2007JA012539

De Franceschi G. & De Santis A. (1994). PASHA: regional long term predictions ionospheric parameters by ACHA. *Annali Di Geofisica* **37**(2): 209 – 220.

Elias A.G., Barbas B.F.D.H., Shibasaki K. & Souza J.R. (2014). Effect of solar cycle 23 in foF2 trend estimation. *Earth, Planets and Space* **66**(1): 1 – 4. DOI: http://doi.org/10.1186/1880-5981-66-111

Floyd L., Newmark J., Cook J., Herring L. & McMullin D. (2005). Solar EUV and UV spectral irradiances and solar indices. *Journal of Atmospheric and Solar-Terrestrial Physics* **67**(1): 3 – 15.

Gulyaeva T.L. (1999). Regional analytical model of ionospheric total electron content: monthly mean and standard deviation. *Radio Science* **34**(6): 1507 – 1512. DOI: http://doi.org/10.1029/1999RS900080

Hedin A.E., Reber C.A., Spencer N.W., Brinton H.C. & Kayser D.C. (1979). Global model of longitude/UT variations in thermospheric composition and temperature based on mass spectrometer data. *Journal of Geophysical Research: Space Physics* **84**(A1): 1 – 9. DOI: http://doi.org/10.1029/JA084iA01p00001

Holt J.M., Zhang S. & Buonsanto M.J. (2002). Regional and local ionospheric models based on Millstone Hill incoherent scatter radar data. *Geophysical Research Letters* **29**(8): 2 – 4.

Ikubanni S.O., Adebesin B.O., Adebiyi S.J. & Adeniyi J.O. (2013). Relationship between F2 layer critical frequency and solar activity indices during different solar epochs. *Indian Journal of Radio and Space Physics* **42**(April): 73 – 81.

Ikubanni S.O. & Adeniyi J.O. (2017). Relationship between ionospheric F2-layer critical frequency, F10.7, and F10.7P around African EIA trough. *Advances in Space Research* **59**(4): 1014 – 1022. DOI: http://doi.org/10.1016/j.asr.2016.11.013

Jaisingh L.R. (2006). *Statistics for the Utterly Confused*, 2nd edition. McGraw-Hill Professional Publishing, NewYork, USA.

Jixiang C. (2006). Using new material to analyze the effect of ionospheric disturbance on short-wave communication. *Proceedings of the 7th International Symposium on Antennas, Propagation and EM Theory*, 26 – 29 October, Guilin, China, pp. 1 – 3. DOI: http://doi.org/10.1109/ISAPE.2006.353509

Kane R.P. (1992). Solar cycle variation of foF2. *Journal of Atmospheric and Terrestrial Physics* **54**: 1201 – 1205.

Kleiber C. (2007). A guide to the dagum distributions. *Modeling Income Distributions and Lorenz Curves. Economic Studies in Equality. Social Exclusion and Well-Being* (ed. D. Chotikapanich), volume 5. Springer, New York, USA.

Lakshmi D.R., Reddy B.M. & Dabas R.S. (1988). On the possible use of recent EUV data for ionospheric predictions. *Journal of Atmospheric and Terrestrial Physics* **50**: 207 – 213.

Legrand J.P. & Simon P.A. (1989). Solar cycle and geomagnetic activity: a review for geophysicists. I - The contributions to geomagnetic activity of shock waves and of the solar wind. II - The solar sources of geomagnetic activity and their links with sunspot cycle activity. *Annales Geophysicae* **7**: 565 – 593.

Liu L., Wan W. & Ning B. (2004). Statistical modeling of ionospheric foF2 over Wuhan. *Radio Science* **39**(RS2013): 1 – 10.
DOI: http://doi.org/10.1029/2003RS003005

Liu L., Wan W., Ning B., Pirog O. & Kurkin V. (2006). Solar activity variations of ionospheric peak electron density. *Journal of Geophysical Research* **111**(April): 1 – 13.
DOI: http://doi.org/10.1029/2006JA011598

Lukianova R. & Mursula K. (2011). Changed relation between sunspot numbers, solar UV/EUV radiation and {TSI} during the declining phase of solar cycle 23. *Journal of Atmospheric and Solar-Terrestrial Physics* **73**(2 – 3): 235 – 240.
DOI: https://doi.org/10.1016/j.jastp.2010.04.002

Maltby P. & Albregtsen F. (1979). Solar cycle variation of sunspot intensity and X-ray bright points. *The Astrophysical Journal* **234**: L147 – L149.
DOI: http://doi.org/10.1086/183127

Maruyama T. (2010). Solar proxies pertaining to empirical ionospheric total electron content models. *Journal of Geophysical Research: Space Physics* **115**(A4): A04306.
DOI: http://doi.org/10.1029/2009JA014890

Mielich J. & Bremer J. (2013). Long-term trends in the ionospheric F2 region with different solar activity indices. *Annales Geophysicae* **31**: 291 – 303.
DOI: http://doi.org/10.5194/angeo-31-291-2013

Mikhailov A.V. & Mikhailov V.V. (1995). Solar cycle variations of annual mean noon foF2. *Advances in Space Research* **15**(2): 79 – 82.

Mushtaq M., Alam S.N., Afridi F.A.K. & Ameen M.A. (2015). Effects of sunspots cycles on diurnal and seasonal trend of foF2. *Journal of GeoSpace Science* **1**(September): 44 – 50.

Ozguc A., Atac T. & Pektas R. (2007). Examination of the solar cycle variation of foF2 for cycles 22 and 23. *Journal of Atmospheric and Solar-Terrestrial Physics* **70**(2008): 268 – 276.
DOI: http://doi.org/10.1016/j.jastp.2007.08.016

Pancheva D. & Mukhtarov P. (1998). A single-station spectral model of the monthly median foF2 and M(3000)F2. *Studia Geophysica et Geodaetica* **42**: 183 – 196.

Penn M.J. & Livingston W. (2006). Temporal changes in sunspot umbral magnetic fields and temperatures. *The Astrophysical Journal* **649**(1): L45 – L48.
DOI: http://doi.org/10.1086/508345

Ramesh K.B. & Rohini V.S. (2008). 1-8 Å Coronal background X-ray emission and the associated indicators of photospheric magnetic activity. *The Astrophysical Journal Letters* **686**(1): L41.

Rao M.S.V.G. & Rao R.S. (1969). The hysteresis variation in F2-layer parameters. *Journal of Atmospheric and Terrestrial Physics* **31**(8): 1119 – 1125.

Rawer K., Bilitza D. & Ramakrishnan S. (1978). Goals and status of the international reference ionosphere. *Reviews of Geophysics* **16**: 177 – 181.

Richards P.G. (2001). Seasonal and solar cycle variations of the ionospheric peak electron density: comparison of measurement and models. *Journal of Geophysical Research: Space Physics* **106**(A7): 12803 – 12819.
DOI: http://doi.org/10.1029/2000JA000365

Rishbeth H. (1998). How the thermospheric circulation affects the ionospheric F2-layer. *Journal of Atmospheric and Solar-Terrestrial Physics* **60**: 1385 – 1402.

Ruiping M., Jiyao X., Wenbin W. & Jiuhou L. (2012). The effect of ~27 day solar rotation on ionospheric F2 region peak densities (N_mF_2). *Journal of Geophysical Research* **117**: 1 – 14.
DOI: http://doi.org/10.1029/2011JA017190

Sams III B.J., Golub L. & Weiss N.O. (1992). X-ray observations of sunspot penumbral structure. *The Astrophysical Journal* **399**: 313 – 317.
DOI: http://doi.org/10.1086/171926

Schunk R.W. & Walker J.C.G. (1973). Theoretical ion densities in the lower ionosphere. *Planetary and Space Science* **21**(11): 1875 – 1896.

Sethi N.K., Goel M.K. & Mahajan K.K. (2002). Solar cycle variations of f_0F_2 from IGY to 1990. *Annales Geophysicae* **20**: 1677 – 1685.

Simon P.A. & Legrand J.P. (1986). Some solar cycle phenomena related to the geomagnetic activity from 1868 to 1980. II - High velocity wind streams and cyclical behavior of poloidal field. *Astronomy and Astrophysics* **155**(2): 227 – 236.

Sizun H. (2003). *Radio Wave Propagation for Telecommunication Applications*, 1st edition. Springer-Verlag, Paris, France.
DOI: http://doi.org/10.1007/b137896

Usoskin I.G. (2017). A history of solar activity over millennia. *Living Reviews in Solar Physics* **14**(1): 1 – 97.
DOI: http://doi.org/10.1007/s41116-017-0006-9

Xu T., Wu Z., Wu J., Wei G. & Feng J. (2008). A single-station spectral model of the monthly median foF2 over Chongqing, China. *Annals of Geophysics* **51**(4): 609 – 618.

Yadav S., Dabas R.S., Das R.M., Upadhayaya A.K. & Sarkar S.K. (2011). Variation of F-region critical frequency (foF2) over equatorial and low-latitude region of the Indian zone during 19th and 20th solar cycle. *Advances in Space Research* **47**(1): 124 – 137.
DOI: http://doi.org/10.1016/j.asr.2010.09.003

Yan X.L., Deng L.H., Qu Z.Q. & Xu C.L. (2011). The phase relation between sunspot numbers and soft X-ray flares. *Astrophysics and Space Science* **333**(1): 11 – 16.

Yanhong C., Weixing W., Libo L. & Libin L. (2002). A statistical TEC model based on the observation at Wuhan Ionospheric Observatory. *Chinese Journal of Space Science* **22**(1): 27 – 35.